論文 Unified Concrete Plasticity Model in Three Dimensional Analysis of Reinforced Concrete Members

Supratic GUPTA *1 & Tada-aki TANABE *2

ABSTRACT: The characteristics of the plasticity model named the Unified Concrete Plasticity Model, proposed by Tanabe. et. al.[1] was modified by Gupta and Tanabe[2,3]. In this paper, this model is applied for the three dimensional finite element analysis RC members and compared with the experimental results. The effect of confinement that cannot be captured in the two dimensional analysis is shown to be properly simulated in the analysis. The effect of tension stiffening effect is implemented and evaluated by comparing a case of beam under two point loading with that of a column. Finally the crack pattern obtained in the beam analysis is also studied.

KEYWORDS: *Concrete, plasticity, 3-D Analysis, Unified Concrete Plasticity Model*

1. INTRODUCTION

Three dimensional finite element analysis of Reinforced Concrete (RC) members is a very complicated matter. Recently a classical plasticity model, named Unified Concrete Plasticity Model was first proposed by Tanabe et. al.[1]. This model is a modified Drucker-Prager model, such that Mohr-Coulomb core matches both at tensile and compressive meridian. This model was later modified by Gupta and Tanabe[2] and it was shown that the first order yield function and the simple damage rule is better[3].

In this paper, after a brief review of unified concrete plasticity model, this model is applied for the three dimensional finite element analysis RC members and compared with the experimental results. The effect of confinement that cannot be captured in the two dimensional analysis is shown to be properly simulated in the analysis. The effect of tension stiffening effect is implemented and evaluated by comparing a case of beam under two point loading with that of a column. Finally the crack pattern obtained in the beam analysis is also studied.

2. THE UNIFIED CONCRETE PLASTICITY MODEL

Figure 1 shows the initial shape of the yield surface of the unified concrete plasticity model. In this paper, the first order yield function given below is used

$$g(\sigma,\omega)=\sqrt{J_2+k_f(1-AA^*/\eta_0)^2}-(k-\alpha_f I_1)=0 \quad (1)$$

$$k_f=\frac{6C\cos\phi}{\sqrt{3}(3+y\sin\phi_1)},\quad \alpha_f=\frac{2\sin\phi}{\sqrt{3}(3+y\sin\phi_1)} \quad (2)$$

$$AA^*=\sqrt{3}c_o\cot\phi_o/\eta_o \quad (3)$$

$$y=\sqrt{a(\cos 3\theta+1.00)+0.01}-1.10,\ a=0.5r^2+2.1r+2.2,$$

$$r=\begin{cases}3.14 & I\le f_c'\\ 2.93\cos\left(\dfrac{f_t-I_1}{f_t-f_c'}\pi\right) & f_c'<I\le f_t\\ 9.0 & I>f_t\end{cases} \quad (4)$$

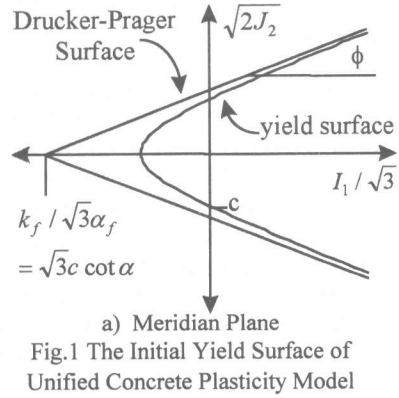

a) Meridian Plane

Fig.1 The Initial Yield Surface of Unified Concrete Plasticity Model

where σ is stress tensor; I_1, J_2 and J_3 are the stress invariants; $\cos 3\theta=(3\sqrt{3}J_3)/(2J_2^{1.5})$ and ϕ_1=14° is a

*1 Department of Civil Eng., Nagoya Institute of Technology, Research Associate, Member of JCI
*2 Department of Civil Eng., Nagoya University, Professor, Member of JCI

material constant. Cohesion c and friction angle ϕ are the most important parameters in this model depending on the damage ω. The initial material parameters defining them are assumed to be constant. The change of frictional angle ϕ and cohesion C are assumed to be different in case of uniaxial tension and uniaxial compression. Based on parameter $X(=I_1/\sqrt{3J_2})$, an appropriate smooth variation between the two zones was proposed[3]. Moreover *tension stiffening* effect requires stress to remain non-zero for RC members, unlike that in plain concrete. Even for compression, it has often been suggested that concrete stress-strain curve actually does not become zero with a constant value after $1.75\,\varepsilon_0$ (ε_0 is the strain at peak stress point for uniaxial compression). Hence, based on material constants ϕ_0, ϕ_f, c_0, η_0 the author propose the following relationship for c and ϕ for appropriate use in analysis of RC members as though other relations can also be considered as shown in Fig. 2.

$$c=\alpha\, c_0 \exp\left[(-m_1\omega)p_1(X)+(-m_2^2\omega^2)p_2(X)\right]+(1-\alpha)c_0,$$

$$\phi=\begin{cases}\phi_0+(\phi_f-\phi_0)\sqrt{(\omega+k)(2-\omega-k)}\,p_2(X) & \omega\le 1\\ \phi_0+(\phi_f-\phi_0)\,p_2(X) & \omega>1\end{cases} \qquad (5)$$

where $k=10^{-3}$ (small value) to avoid the singularity at $\omega=0$ and

$$\{p_1(X)\quad p_2(X)\}=\begin{cases}0 & \\ \frac{1}{2}\cos\left(\frac{X-a1}{a2-a1}\pi\right)+\frac{1}{2} & \\ 1 & \end{cases} \qquad (6)$$

$$\begin{matrix}1 & X\le a1\\ \frac{-1}{2}\cos\left(\frac{X-a1}{a2-a1}\pi\right)+\frac{1}{2} & a1<X\le a2\\ 0 & X>a2\end{matrix}$$

where a1= -1 and a2= -0.15 was found to be appropriate[3,4] for the stress-strain relations for concrete.

The *simple damage* model is assumed as

$$d\omega=\beta' d\varepsilon^p=\beta' d\lambda \qquad (7)$$

where $d\lambda$ is scalar plastic multiplier assumed equal to plastic strain.

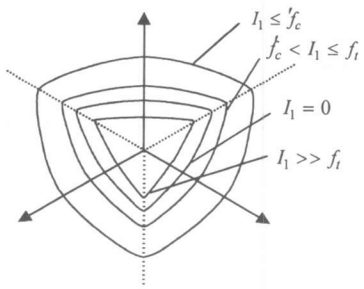

b) Diviatoric Plane

Fig.1 The Initial Yield Surface of Unified Concrete Plasticity Model

$$c=\alpha\, c_0 \exp\left[(-m_1\omega)p_1(X)+(-m_2^2\omega^2)p_2(X)\right]+m_3\omega+(1-\alpha)c_0$$

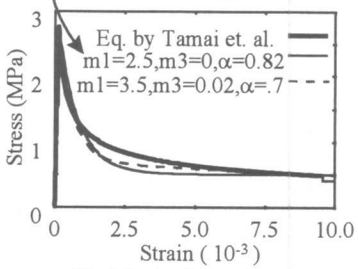

Fig.2 Uniaxil Tension

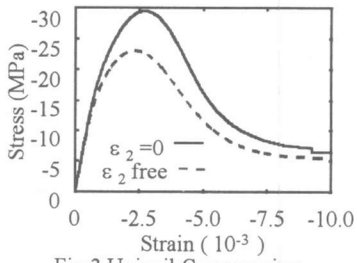

Fig.3 Uniaxil Compression

Fig. 2 shows stress strain response using a generalized variation for cohesion c under uniaxial tension and the relation proposed by Tamai et. al.[4] (also adopted by Tsu[5]) for proper simulation of tension stiffening effect within reasonable limits. Fig. 3 shows the uniaxial compression behavior with and without lateral strain ε_2 and show quite acceptable stress-strain behavior with increased strength and ductility.

3. REINFORCEMENT: STRESS STRAIN RELATIONSHIP

Typical stress-strain relationship for reinforcement obtained by uniaxial tension shows initial linear elastic portion, a yield plateau with negligible increase of stress, a strain hardening range where stress increases and finally a stage where stress drops until fracture occurs. The most often used curves are bilinear, trilinear and complete curve till the strain hardening range.

Recently, Hsu[5] and his colleagues have proposed the use of bilinear curve (or single equivalent curve) with *lower apparent yield stress* and *higher post yield slope* for proper simulation of the average stress-strain relationship in a reinforced concrete member due to tension stiffening effect based on experiments on thin panel under uniaxial tension to consider the tension stiffening effect. They found that the apparent yield stress and slope to be dependent on the reinforcement ratio. However, in these experiments, multiple cracks

are generated and followed by a stage with stable crack configuration.

Now would these models that were derived based on experiments on thin panels be applicable to RC members like columns and beams? In the case of the beam under two point loading, the bottom sections is cracked under tension. Each crack propagates(with increasing area of cracked surface) with a varying distribution of strain along the crack. However in the case of thin panels, the cracks were generally through with uniform strain distribution cracks across the cross-section. Hence the applicability of this model is a question of further research. In this paper different models for the stress strain relation for reinforcement are implemented to test the applicability of the tension stiffening effect.

4. A RC BEAM UNDER TWO POINT AND A RC COLUMN UNDER LATERAL LOADING

Table 1: Parameters for the Concrete Constitutive Model

	E_c(MPa)	f_t (MPa)	f_c' (MPa)	c_o(MPa)	ϕ_1
Beam	34600	3.15	33.75	22.58	14°
Column	34960	3.23	35	24.58	14.3

Fig. 4a shows the dimensions of the beam under two point loading (load controlled) with enough stirrups to cause bending failure carried out in Nagoya University, Japan as a part of regular yearly educational activity. Fig. 5 shows a column under lateral load with controlled displacement[6]. The average of two cylinder strength was f_c' =33.75 MPa and 35 MPa respectively. Based on this, E_c and f_t (mean value) are calculated according to the CEB-FIP Model Code -90[7]. Material parameters are chosen to satisfy Kupfer's experimental results[8] and stress strain curve of concrete under tension to simulate tension stiffening effect. The selected parameters are shown in Table 1 and rest of the parameters which were assumed equal in the two cases are μ=0.22, $\phi_o = 5°$, $\phi_f = 36°$, m_1 =4.0, m_2 =0.83, η_o =7.0 MPa, k = 1.0 x 10^{-3}, ω_f =1.0, $\beta' = 35$, $\gamma = 0.92$, a1= -1.0 and a2= -0.15.

Table 2: Parameters for Reinforcements for the beam

Case	f_y(MPa)	slope(x Es)	f_{y1}(MPa)	slope(xEs)
A	370.0	0.0001	-	-
B	323.4	0.00785	-	-
C	323.4	0.00785	370.0	0.0001

For the beam, in drawing the load-displacement diagram of the experiment, the displacement at the support due support shrinkage is also taken into consideration. Fig. 4b shows the finite element mesh of the quarter section of the beam that is taken for the analysis. As necessary, X or Y direction displacements are restrained for all points in the two symmetry section. In this case, all sections are assumed to have uniform lateral reinforcement. Three cases, with the three different stress-strain relationship for reinforcement with elastic modulus of elasticity Es=210000 MPa, are considered in the analysis as shown in Table 2 or Fig.6 where E_s is the modulus of elasticity in the elastic zone. In case A, we take a bilinear elastic - perfectly plastic curve (post - yield slope

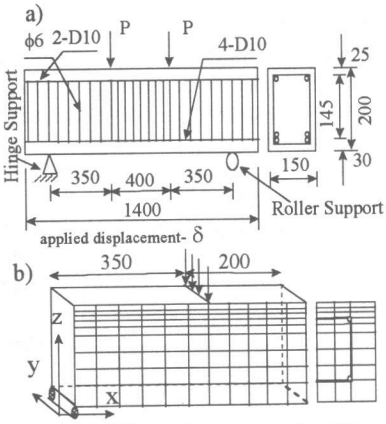

Fig. 4: Dimension and mesh of the Beam for Bending Failure in mm

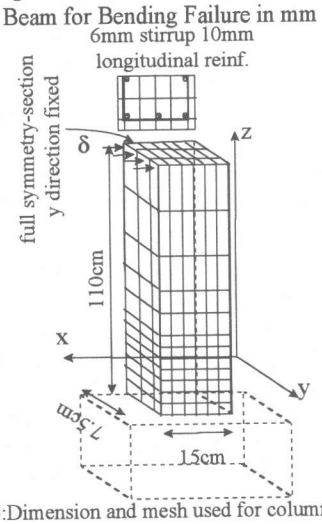

Fig.5:Dimension and mesh used for column

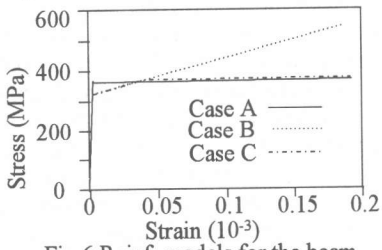

Fig.6 Reinf. models for the beam

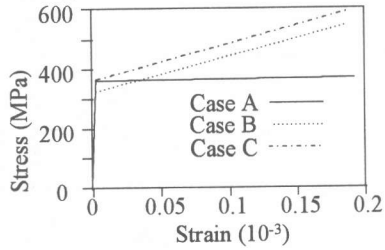

Fig .7: Reinf. models for the column

= 0.01% of E_s is taken for stability of the analysis). In case B, we take a bilinear curve with approximate apparent yield stress and higher slope to simulate tension stiffening effect. In case C, we take trilinear curve with case B type bilinear curve in the beginning and change to case A type curve (with yield stress of f_{y1} and post yield slope of 0.01% of E_s)at the intersection point.

For the column, the dimension and details of the specimen and the mesh selected are shown in Fig. 5. The base is not taken into consideration due to computer limitation. Half section is taken for analysis. Hence the y direction is restrained for all points in the symmetry section. Three cases with different stress strain behavior of reinforcement are considered. For case A, yield strength with post yield slope of $0.0001E_y$ was used to maintain stability in the calculation. In Case B, the tension stiffening effect is incorporated approximately by adopting appropriate lower apparent yield stress and higher apparent post yield slope. In Case C, we just incorporate the slope as case B , but use f_y = 380 MPa in place of f_y^*.

Table 3: Parameter for Reinforcement for Cantilever

Case	f_y^* (MPa)	slope(xEs)
A	380.0	0.0001
B	332.2	0.00785
C	380.0	0.00785

4.1 EVALUATION OF IMPLEMENTATION OF TENSION STIFFENING EFFECT

From the above calculations in beam under two point loading or column under lateral loading a few interesting observations can be made.

In the *case of beam*, the peak strength is reached when the reinforcement yields when the elastic-perfectly plastic case A is considered and matched the peak strength of the experiment. However, in the experiment, when the reinforcement yielded, the load was lower followed by a gradual hardening before the load - displacement diagram reached the peak. This behavior is correctly predicted when the tension stiffening effect (case B and C) with lowered yield stress was implemented. Even though in the *case of column*, case B and C resembled the experimental load deflection diagram better than the elastic-perfectly plastic case A. However, case C without lowered apparent yield stress provided better load-deflection diagram than case B with lowered apparent yield stress. The possible reason lies in the

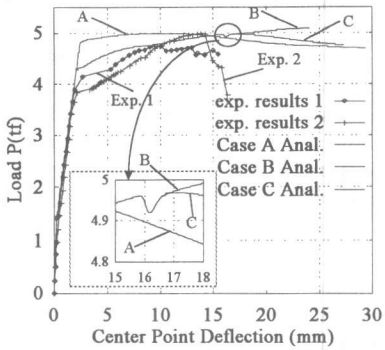

Fig. 8: Load deflection behavior for column under two point loading

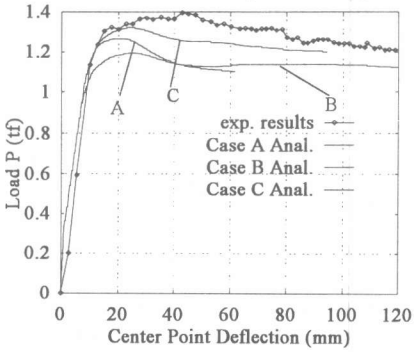

Fig. 9: Load deflection behaviour of column underlateral load

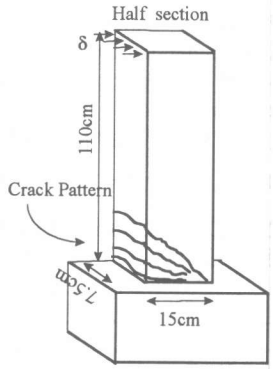

Fig. 10: Crack patterm for the column

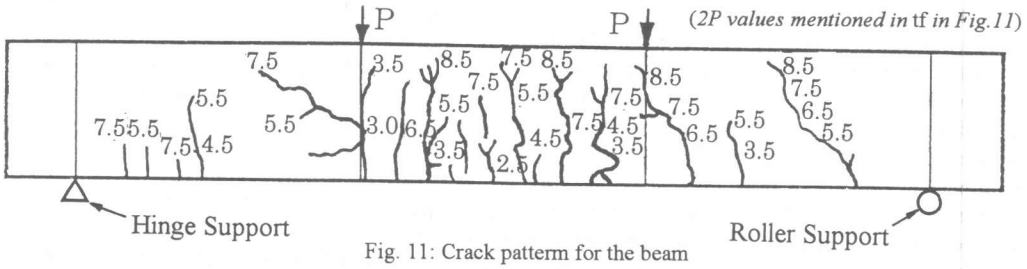

Fig. 11: Crack patterm for the beam

fracture process in the cases. In the case of the column (Fig. 10), the crack zone was very small. However in case of the beam(Fig. 11), the crack zone was wide and cracks appear at regular interval. Hence reinforcement might have indeed yielded in multiple positions in the beam simulating tension stiffening effect properly where as in the column it yielded only in a small zone at the bottom.

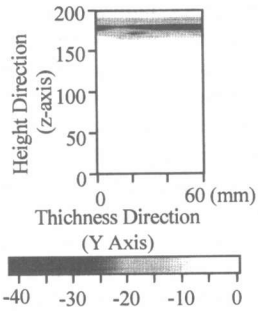

Fig. 12: σ_x distribution in central Section

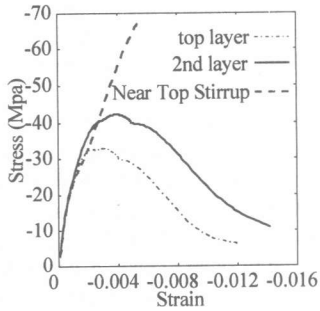

Fig. 13: Confinement effect in σ_x-ε_x relation

The abrupt failure noted in the beam could not be simulated. Implementation of case B of the beam resulted in increasing slope. The decrease in load do not occur as the stress in the reinforcement keeps increasing. Use of intermediate relationship (case C) resulted in decrease in load. The author checked the effect of imposing symmetry by one forth beam analysis by adopting half beam section and found similar results(not shown here). However as we can see in the magnified zone of Fig. 8 that there is a sharp drop in load. The reason behind this was found when we studied the incremental strain $\Delta\varepsilon_x$ in the localized crack that developed as shown in Fig. 15. The description of the figure is same as Fig. 14 as described in next section. The difference in the load deflection behavior in the experimental result where the column showed ductile behavior where as the beam showed brittle behavior in the last stage is strange. The reason could be because the column was tested in displacement controlled manner where the beam was experimented under load controlled(hand control) manner. The authors intends to implement large deflection small strain theory and beam element for reinforcement in compression to simulate buckling of the reinforcement in future to further investigate the failure of beams in the final stage to get a more realistic model for the reinforcement.

All dimensions in Fig. 14 and 15 are in meter

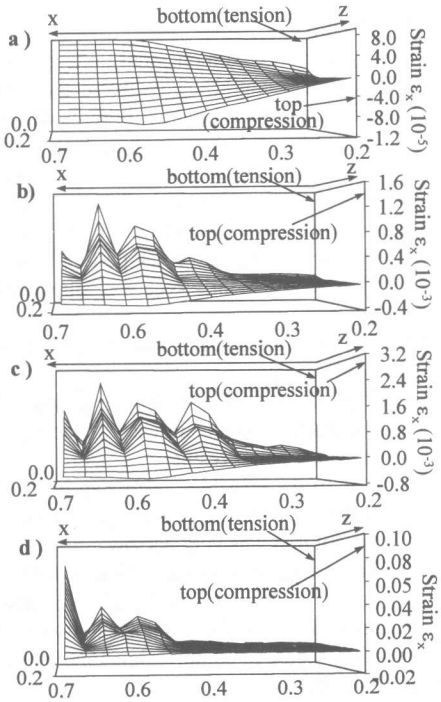

Fig.14: Strain ε_x in x-z plane along the length of the beam showing cracks at different stages

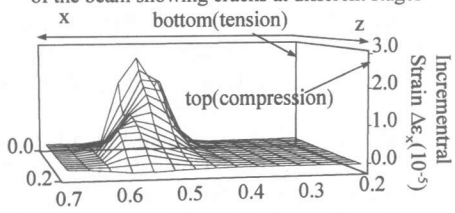

Fig.15: Incrementral Strain $\Delta\varepsilon_x$ in x-z plane along the length of the beam showing localized crack

4.2 DAMAGE PHENOMENON FOR THE BEAM

The concrete stress distribution at the central section at a later stage is shown in Fig. 12. We can see that bottom part of the section has cracked, where as top part has already crushed. The part near the stirrup showed high confinement effect where the peak load and ductility increased a lot as can also be seen in Fig. 13. The top layer provided a stress-strain behavior quite similar to the uniaxial compression case. behavior (Fig. 12) observed in the *central section* was quite reasonable at a final stage of the calculation for Case C of the beam. The bottom section is fully cracked and the top part is crushed where as region near the reinforcement show higher strength due to confinement. The effect of confinement on the stress-strain behavior in the second layer and in the layer near the stirrup is shown in Fig. 13 which shows increased peak and ductility.

To understand the condition of the cracks, Figure 14 shows the ε_x strain distribution in the x-z plane at different stages for the beam. It is a surface plot where the axis in the depth of the paper direction represent the height of the beam(z direction). x direction is along the length of the beam. Figure 14 shows wave like distribution of tensile strain. This represent occurrence of multiple discrete crack in the analysis. This occurred because the eight nodded element can only show linear strain. This problem can be removed by using higher order element. However, looking from another point of view, this simulation of multiple crack can be called more realistic. In the experiment, we also get multiple distinct cracks.

If we notice the crack pattern of the experiment (Fig. 11), it can be observed that the central cracks grows at a later stage. Finally, strain localization occurs and the central crack opened up. This results in closing of other cracks. A phenomenon, quite similar to this, was observed in the analysis also. In Fig. 14, the strain distribution in a section (x-z plane) at different stages shows four major crack. The forth crack is outside the central zone(Fig. 14b and c) as is observed in the experiment. This represent the shear crack. In the beginning, the central crack is not the dominating crack. However in the final stage(Fig. 14d), stain localization occurs at the center of the beam and the central crack open up. The fourth crack or the shear crack closed at this stage. The strain in the other two crack also decreases.

6. CONCLUSION

In this paper, three dimensional finite element analysis of two cases of a beam under two point loading and column under lateral loading were carried out. The aim of the paper was to check the applicability of unified concrete plasticity model in three dimensional analysis of RC members. There are also some other calculations of beam failing in shear that were also successfully carried out and not reported here due to space limitation. After carrying out these calculations, we can make the following conclusion.

a) The unified concrete plasticity model is able to satisfactorily simulate the experimental results.
b) The stress-strain relationship was simulated properly and it reflected well in the comparison of the development of the crack pattern between the experiment and the analysis.
c) The confinement effect was simulated well in this analysis as shown in the stress in the inner layer.
d) Implementation of tension stiffening effect in the reinforcement effect the load deflection diagram considerably.
e) Implementation of the higher post-yield slope for the reinforcement provide better results for both the cases, however in case of the column, implementation without lowered apparent yield stress provided better results.
f) One of the possible reason can be the fact that there was a wide range of uniform multiple crack pattern in the case of beam providing a proper tension stiffening effect where as the crack zone in the column was very narrow.
g) The effect of implementation of tension stiffening effect should be studied in further details. We cannot really conclude based on comparison of just these two cases.

The author feel that there is a necessity to introduce beam element for the reinforcement to simulate the buckling that occurs in compression zone at the final stage of failure.

REFERENCES

1. Tanabe,T., Wu,Z. and Yu,G., "A Unified Plastic Model for Concrete" JSCE,Vol.24,No.296, Aug.,1994,pp.21-29.
2. Gupta, S. and Tanabe, T., "Investigation and Modification of the Characteristics of the Unified Concrete Plasticity Model", JCI,1995,pp.1305-1310.
3. Gupta, S. and Tanabe, T., "Modified Unified Concrete Plasticity Model and its variations", JCI, Vol.18, No.2., 1996, pp.425-430.
4. Tamai, S., Shima, H., Izumo,J. and Okamura, H. 'Average Stress-Strain Relationship in Post Yield Range of Steel Bar in Concrete', Concrete Lib. JSCE, No. 11, June 1988, pp.117-129.
5. Thomas T.C.Hsu, 1993, "Unified Theory of Reinforced Concrete", CRC Press.
6. Hirasawa, I., Kanoh, M. and Fujishiro. M., "Basic Test on Dynamic Strength of R/C Square Columns under Biaxial Bending", The Society of Material Science, JP.,Vol.45, No. 4, pp. 423~429, April 1996.
7. CEB-FIP Model Code -90,Comite Euro-Int. Du Beton, Publisher by Thomas Telford , pp 34-42.
8. Kupfer, H, Hilsdrof, H.K. and Rusch,H., "Behavior of concrete under Biaxial stress", ACI, Vol.66,No.8, Aug.,1969,pp.656-636.